# Silk Bionanocomposites for Organic Dye Absorption and Degradation

Cristina Belda Marín, Christophe Egles, Jessem Landoulsi, Erwann Guénin

applied sciences

MDPI

*Article*

# Silk Bionanocomposites for Organic Dye Absorption and Degradation

**Cristina Belda Marín [1,2], Christophe Egles [3,†], Jessem Landoulsi [2] and Erwann Guénin [1,*]**

[1] Université de Technologie de Compiègne, ESCOM, TIMR (Integrated Transformations of Renewable Matter), Centre de Recherche Royallieu, CEDEX CS 60319, 60203 Compiègne, France
[2] Sorbonne Université, CNRS, Laboratoire de Réactivité de Surface, 4 Place Jussieu, 75252 Paris, France
[3] Université de Technologie de Compiègne, CNRS, Biomechanics and Bioengineering, Centre de Recherche Royallieu, CEDEX CS 60319, 60203 Compiègne, France
* Correspondence: erwann.guenin@utc.fr
† Current address: Normandie Université, UNIROUEN, INSA Rouen, CNRS, PBS (UMR 6270), 55 Rue Saint-Germain, 27000 Évreux, France.

**Abstract:** Organic dyes are extensively used in the textile, paper and paint industries, among others. However, the lack of efficient treatment of disposals leads to the release of these toxic molecules into the environment, which has an enormous impact on living organisms. Dye absorption is the most common approach used to tackle this problem. However, the ideal solution should include dye degradation and absorbent regeneration, reducing the environmental impact of the procedure. Dye degradation can be achieved by catalysis. Recently, silk fibroin (SF) has been shown to have incredible absorbent properties. Herein, we characterized the capacity of SF hydrogels to absorb methylene blue (MB), an extensively used cationic organic dye. Moreover, the effect of a pretreatment of the SF hydrogel at different pH and ionic environments is also studied. Interestingly, opposite behaviors are observed when absorbing MB or brilliant blue (an anionic dye), suggesting an electrostatic-based interaction. Furthermore, the regeneration of a MB-saturated SF hydrogel by immersion in acidic pH and its further reuse were evaluated. Finally, the SF hydrogel was coupled with a gold nanoparticle catalyst, which resulted in a material able to absorb and catalyze the MB reduction by sodium borohydride in situ, leading to dye degradation. Overall, this work presents a biodegradable reusable material able to absorb and reduce MB in aqueous media.

**Keywords:** silk; hydrogel; methylene blue; adsorption; nanocomposite; gold nanoparticle; catalysis; depollution



**Citation:** Belda Marín, C.; Egles, C.; Landoulsi, J.; Guénin, E. Silk Bionanocomposites for Organic Dye Absorption and Degradation. *Appl. Sci.* **2022**, *12*, 9152. https://doi.org/10.3390/app12189152

Academic Editors: Raed Abu-Reziq

Received: 30 July 2022
Accepted: 4 September 2022
Published: 13 September 2022



## 1. Introduction

Extensive global industrialization has raised many concerns about environmental pollution. In particular, industrial wastes are poorly treated before disposal. Residual waters flow into rivers, lakes, underground water and seawaters containing a great number of pollutants [1]. The presence of pollutants such as heavy metal ions and organic dyes in the environment strongly affects the ecosystem and consequently human health [1–3]. Furthermore, water is an essential resource for life, and the amount of drinkable water is in constant decrease due to the increase in worldwide population and the resulting expansion of pollution.

Organic dyes are widely used in the textile, paper, paint, cosmetics, printing, plastics and pharmaceutical industries, among others [4,5]. Yet, several organic dyes are greatly toxic for living organisms and are potentially carcinogenic and mutagenic [2,6]. In the environment, these molecules are poorly or not completely degraded due to their complex aromatic structures. Their relative stability therefore drives environmental accumulation, where small modifications or combinations with other molecules can further increase their toxicity [7]. Methylene blue (MB) is a cationic organic dye extensively used by industry, and it is therefore used as model dye for many depollution applications. When ingested, MB may indeed cause nausea, vomiting or gastritis [8].

Extensive studies have been conducted on the development of efficient water depollution methods. The latter include precipitation, flocculation, ion exchange, filtration, adsorption and photodegradation, which have been successfully used [5,8,9]. Depollution through adsorption remains, however, the most widely used method due to its cost effectiveness and simplicity [10]. Ideal adsorbent materials should have high adsorption capacities, biodegradability, ease regeneration and recyclability.

In this context, silk fibroin (SF)-based materials have been developed in applications dealing with the depollution of organic and inorganic compounds [11–17]. Silk is a natural biopolymer produced by many members of the arthropod's family. Because of its biocompatibility, biodegradability and tunable mechanical properties [18–23], silk-based materials have been developed and applications for them have been found in many fields such as medicine, catalysis and depollution. *Bombyx mori* worm's silk is the most abundant due to worm domestication and its mass production mainly for the textile industry. *B. mori* silk is composed of two proteins: fibroin and sericin. Fibroin forms the core structure of silk threads and is surrounded by sericin. Traditional procedures, mainly thread production for the textile industry, use a degumming process that results in the removal of the surrounding sericin. Therefore, most of the silk materials are composed only of SF. Recently, many different SF materials have been developed, including electrospun mats, additive manufacturing, hydrogels and microspheres, among others [24]. Interestingly, the absorption capacity of SF materials has been scarcely shown in the literature. Gao et al. showed the potential of silk electrospun membranes for air filtration [25]. The produced filters were able to remove from air up to 99.99% of the particles between 0.3–10 μm, while showing a decreased pressure drop in comparison with the state-of-the-art materials. Another study proved the combination of SF with hydroxyapatite to be efficient for water filtration and purification [12]. The described material was able to remove dyes and heavy metal ions from solutions, which cannot be achieved with conventional nanofiltration membranes. Finally, silk hydrogels obtained from recombinant bee silks produced in *E. coli* have also been shown to absorb metal macrocycles, organic dyes and nanoparticles [26,27].

However, the main issue with the adsorption approaches is related to the fact that pollutants are only removed from the environment but not eliminated. Activated carbon is the most largely used adsorbent material. When it reaches its maximum adsorbent capacity, this material is either degraded *a posteriori* by pyrolysis, an energy-consuming process producing a high amount of $CO_2$, or directly discarded into landfills, thus contributing to further pollution [28]. Accordingly, an adsorbent-based approach requires the combination with a non-pollutant dye/material degradation strategy.

To overcome this issue, two main strategies have been developed: material regeneration and dye degradation. The regeneration of the material allows its reutilization, thus increasing its lifetime and performance. Dye degradation can be achieved through catalysis. In particular, the use of nanoparticles (NPs), which exhibit a high surface-to-volume ratio, has been widely explored to this end as lower amounts of catalyst are required. A variety of NPs have been used for dye degradation including silver, platinum, iron, palladium and gold [29–34]. Although palladium NPs are probably the most well-know nanocatalyst, their expensiveness and toxicity reduces their interest in depollution applications. In contrast, gold NPs (Au NPs) have a reduced toxicity and better stability over time [35,36].

Herein, we report the use of SF-Au NPs bionanocomposite for a combined adsorption and degradation of a MB. The adsorption capacities of SF hydrogels are assessed by monitoring the evolution of MB amounts in aqueous media. The hydrogels were also pre-incubated in solution with different pH and ionic strength to investigate the possible changes in their adsorption capacities. The regeneration of the studied materials and their further recycling was also studied. Particular attention was given to the association of SF materials and Au NPs to combine adsorbent capacity and dye-degradation catalysis processes.

## 2. Materials and Methods

### 2.1. Materials

Methylene blue (MB, M9140), brilliant blue (BB, erioglaucine disodium salt, 861146), NaCl, $NaBH_4$, Lithium bromide (LiBr, reagent plus ≥ 99.9%), horseradish peroxidase type VI (HRP, P8375), PDMS (Sylgard 184), 2,2′-Azino-bis (3-Ethylbenzthiazoline-6-Sulfonic Acid) (ABTS) were purchased form Sigma-Aldrich (St. Quentin Fallavier, France) with 98.5% minimum purity.

HMBP-C≡CH (1-hydroxy-1-phosphonohept-6-ynyl) phosphonic acid was synthesized as previously reported [37]. Hydrogen tetrachloroaurate (III) ($HAuCl_4$, $3H_2O$, ≥99.9%), sodium ascorbate, sodium carbonate ($Na_2CO_3$, 99.8%, anhydrous) and hydrogen peroxide ($H_2O_2$, 35 wt.%) were purchased from Fisher Scientific.

### 2.2. Silk Fibroin Extraction

Silk fibroin (SF) dispersion was obtained as previously described elsewhere [38]. Briefly, *Bombyx mori* silk cocoons were cut into small pieces and boiled for 30 min in 0.02 M $Na_2CO_3$ solution to remove sericin. Fibers were rinsed three times with abundant demineralized water, dried and dissolved in a 9.3 M LiBr solution. The resultant dispersion was then dialyzed against demineralized water for 48 h, in a 3500 molecular weight cut off (MWCO) dialysis cassette. Insoluble residues were removed by centrifuging twice at 9000 rpm for 20 min. SF dispersion was diluted to 6 wt.% and stored at 4 °C before use.

### 2.3. Gold Nanoparticle Synthesis

Gold nanoparticles (Au NPs) were synthesized by following the procedure described in previous work [39]. Briefly, 19 mL of demineralized water were mixed with 250 µL of $HAuCl_4$ (20 mM) and 500 µL of HMBP-C≡CH dispersed in water solution (40 mM) previously adjusted at pH = 10. The solution was placed under vigorous stirring at room temperature (RT) and 55 µL of sodium ascorbate (17.6 mg $L^{-1}$) were added. The reaction was considered finished after 30 min. Suspensions were dialyzed (MWCO 100 kDa) then stored at 4 °C before use.

### 2.4. SF-Au NPs Bionanocomposite

SF hydrogels were formed by mixing 6% (wt.%) SF dispersion with water or 0.25 mM Au NPs dispersion in a 1:1.6 ratio. Gelation was induced by adding 10 µL of HRP (1 unit $\mu L^{-1}$) and 10 µL of $H_2O_2$ 1% following the protocol originally described by Partlow et al. [40]. Gelation was carried out in PDMS molds for easy post manipulation and in a glass desiccator in the presence of two water-containing beakers to increase humidity and avoid evaporation. Gelation time was set to 72 h. For the sake of comparison, SF hydrogel without Au NPs was also prepared following the procedure described above.

### 2.5. Dye Adsorption

SF hydrogels (0.034 g of SF per hydrogel) were immersed in 15 mL of pH = 7 MB (10 mg $L^{-1}$) or BB (10 mg $L^{-1}$) solution and placed in an orbital shaker at RT.

### 2.6. Adsorption Isotherms

The adsorption capacity of SF sponges and swollen hydrogels were evaluated by immersing the samples in 15 mL of MB solution (10–200 mg $L^{-1}$) under stirring at RT for 48 h to reach the equilibrium concentration ($C_e$; MB concentration in the solution at the equilibrium state). After incubation, the absorbance at 664 nm of the solution was measured. $C_e$ and the adsorption capacity ($q_e$; mg $g^{-1}$; mass of adsorbed MB (mg) per mass of adsorbent (g)) parameters were calculated for each point. Results were fitted with the Langmuir, Freundlich and Temkin adsorption models as these models are widely used in

the literature for similar systems [10,15,41–44]. The Langmuir model can be described by Equation (1).

$$q_e = \frac{q_m K_L C_e}{1 + K_L C_e} \quad (1)$$

This equation can be linearized as follows:

$$\frac{C_e}{q_e} = \frac{1}{q_m K_L} + \frac{1}{q_m} \times C_e \quad (2)$$

The Freundlich experimental model can be described by the following equation:

$$q_e = K_F C_e^{1/n} \quad (3)$$

It can be linearized as:

$$\ln(q_e) = \ln(K_F) + \frac{1}{n} \ln(C_e) \quad (4)$$

The Temkin model can be described by Equation (5).

$$q_e = \frac{RT}{b_T} \ln(K_T C_e) \quad (5)$$

This equation can be linearized as follows:

$$q_e = \frac{RT}{b_T} \ln(K_T) + \frac{RT}{b_T} \ln(C_e) \quad (6)$$

where $q_e$ is the adsorption capacity (mg MB g adsorbent$^{-1}$); $q_m$ the maximum adsorption capacity (mg g$^{-1}$); $C_e$ the MB concentration at the equilibrium state (mg L$^{-1}$); n represents the heterogeneity of the adsorbent; $K_L$, $K_F$ and $K_T$ are the adsorption constants (L mg$^{-1}$) of the Langmuir, Freundlich and Temkin models, respectively. $T$ is the absolute temperature in Kelvin ($K$), $R$ is the universal gas constant, 8.314 J mol$^{-1}$ K$^{-1}$, $b_T$ is the constant related to the heat of adsorption indicating the variation of adsorption energy (J mol$^{-1}$).

### *2.7. Materials Pretreatment*

The effect of pH (3.5, 5 and 8) and ion pretreatments (0.6 M, NaCl) on the adsorption capacities of SF hydrogels were evaluated. After gelation, samples were immersed in demineralized water for 48 h at RT for complete swelling. Swollen materials were then treated by immersion into a given pretreatment solution for an additional 48 h. Pretreatment solution pH were adjusted using 1 M HCl/NaOH solutions. Prior to MB adsorption, materials were abundantly rinsed with demineralized water (Figure 1).

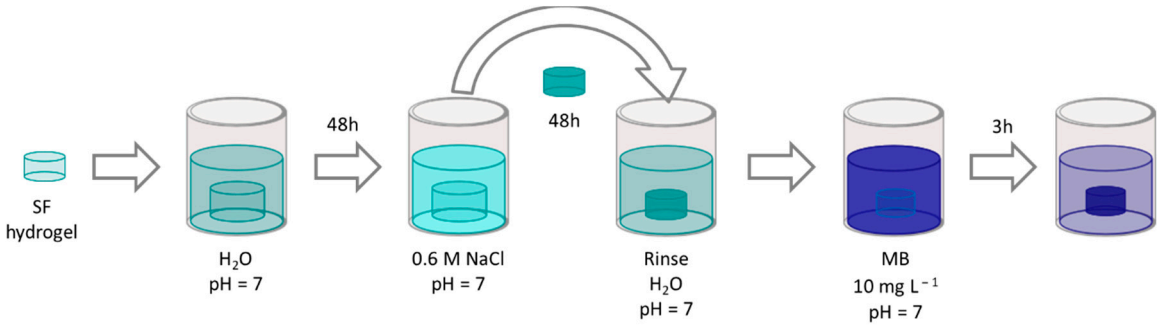


**Figure 1.** Schema of the procedure followed to evaluate the effect of salt pretreatment on the SF hydrogel MB adsorption capacity. After formation, the hydrogel is immersed in water for swelling, then in a 0.6 M NaCl solution until hydrogel saturation (6 days). The hydrogel is then rinsed and immersed in 10 mg L$^{-1}$ MB solution for MB absorption.

### *2.8. MB Release*

After their preparation and subsequent immersion in aqueous solution (water, pH adjusted at 7) for 48 h, the hydrogels were immersed in MB solutions (10 mg $L^{-1}$, pH = 7) for 6 days. MB release was performed by immerging MB-saturated SF materials in aqueous solution (pH 3, $10^{-3}$ M HCl) and monitoring by spectrophotometry at 664 nm. The procedure is presented in Figure 2.

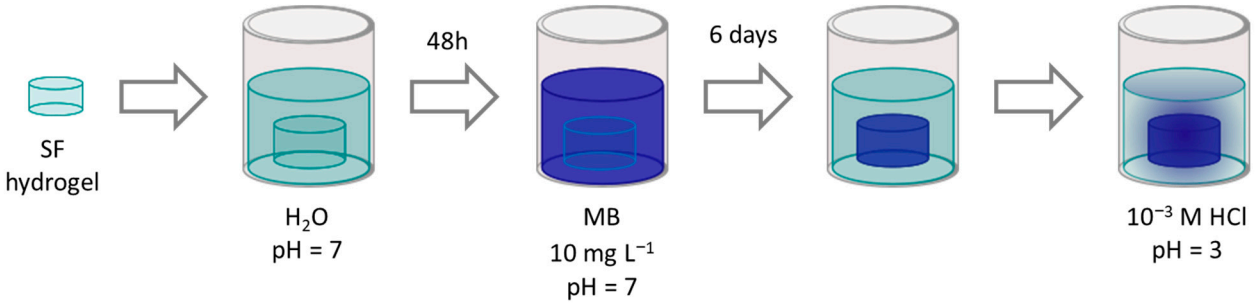


**Figure 2.** Schema of the procedure followed to evaluate SF hydrogel MB release. After formation, the hydrogel is immersed in water for swelling, then in a MB solution until hydrogel saturation (6 days). The MB-saturated hydrogel is then immersed in $10^{-3}$ M HCl solution for MB release.

### *2.9. Catalytic Activity*

1.5 mL SF-Au NPs hydrogel bionanocomposites (0.034 g SF and ~0.15 mM final Au NPs concentration) were placed in water to allow complete swelling for 48 h. Hydrogels were immersed in 5 mL of MB solution (10, 50 or 100 mg $L^{-1}$) and 500 µL of 1 M $NaBH_4$ were added. Reaction was carried out under constant stirring and a 2 mL aliquot was taken out at a given time for absorbance measurement (λ = 664 nm). Due to the high speed of the reaction, it was not possible to measure the absorbance at several time points for a single reaction. Therefore, four different reactions were carried out, and a single time point measurement was performed.

The possibility to further chemically reduce MB using the same SF-Au NPs hydrogel was evaluated by adding 1 mL of MB (10 mg $L^{-1}$) and 500 µL of 1 M $NaBH_4$ after complete MB reduction. This procedure was repeated up to 15 times by simply washing the hydrogel with fresh water and adding fresh MB and $NaBH_4$ solution. The same procedure was repeated three times using a 100 mg $L^{-1}$ MB solution.

## 3. Results and Discussion

### *3.1. Silk Fibroin Materials Preparation*

SF hydrogels were successfully prepared following the procedure described elsewhere, which consists in inducing the gelation by horseradish peroxidase (HRP) and $H_2O_2$ [40]. Thus obtained, the hydrogels were further characterized by scanning electron microscope (SEM) and confocal microscopy. Figure 3A shows the expected porous structure of the freeze-dried hydrogels with a diameter of pores ranging from 5 to 40 µm. Hydrogel macroporous structure was confirmed by confocal imaging in their wet state (Figure 3B).

Adsorption capacities were evaluated by immersing SF hydrogels in MB solutions ranging from 10–200 mg $L^{-1}$ for 48 h to reach the equilibrium concentration ($C_e$; MB concentration in the solution at the equilibrium state). Three well-known adsorption models were used to describe the adsorption mechanism. The Langmuir model is a theoretical model based on the fact that adsorption takes place on the surface in the form of a monolayer in a reversible way. In contrast, the Freundlich model is an empirical model in which multilayered adsorption is considered. As for the Temkin model, the interaction between adsorbent and adsorbate is considered. The model assumes, indeed, that the heat due to the adsorption process will decrease due to the adsorbent–adsorbate interaction. Table 1 summarizes the values of each parameter extracted from the Langmuir,

Freundlich and Temkin models as well as the correlation coefficient value $R^2$. The results were satisfactorily consistent with the Langmuir model (Figure 4) in agreement with most of the studies on organic dye adsorption found in the literature [15,45–47].

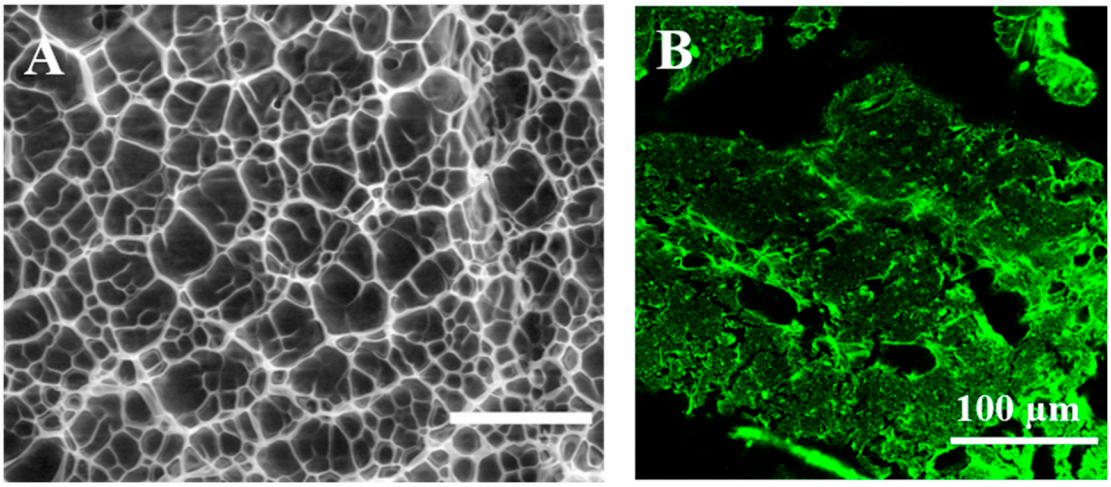


**Figure 3.** Silk hydrogel structure evaluation in a freeze-dried state by SEM (**A**) and in a wet state by confocal microscopy (**B**).

**Table 1.** Value for the parameters in the Langmuir, Freundlich and Temkin adsorption models and the correlation factor with the experimental data.

| **Langmuir** | | | **Freundlich** | | | **Temkin** | | |
|---|---|---|---|---|---|---|---|---|
| $q_m$ | $K_L$ | $R^2$ | 1/n | $K_F$ | $R^2$ | $b_T$ | $K_T$ | $R^2$ |
| 25.77 | 0.23 | 0.996 | 0.34 | 6.33 | 0.624 | 638.29 | 8.75 | 0.8223 |

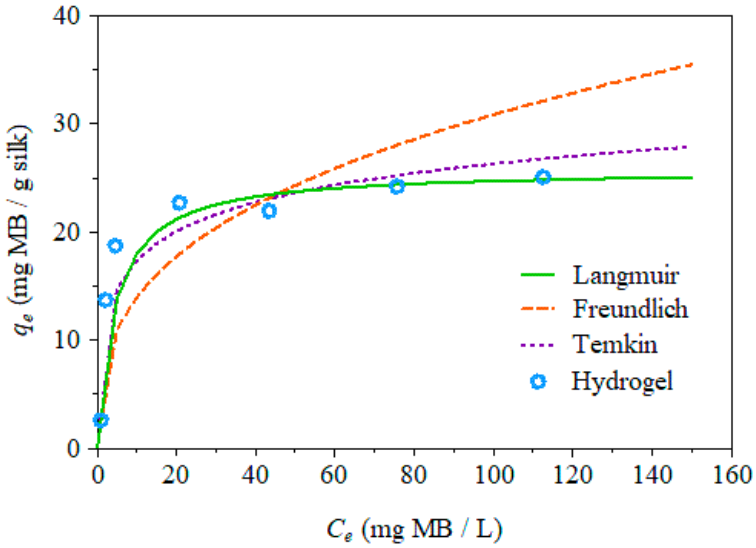


**Figure 4.** Methylene blue adsorption by SF hydrogels fitted to the Langmuir and Freundlich adsorption models. Best fit is found with the Langmuir model.

We hypothesized that the adsorption of MB was mainly due to electrostatic interactions. SF hydrogels were tested under three different conditions to evaluate this hypothesis: (i) the pretreatment of SF materials with different pH solutions or (ii) with sodium chloride and (iii) the use of an anionic dye.

### 3.2. Effect of pH

SF being a protein, its overall charge is pH dependent and can therefore be modulated by varying this factor. In contrast, the MB molecule is positively charged over a wide range of pH as its pKa values are 2.6 and 11.2. To validate our hypothesis based on an electrostatic interaction, the effect of pH pretreatment was studied. To this end, hydrogel samples were immersed for 48 h in solutions at pH of 3.5, 5 and 8. The pH was adjusted with HCl or NaOH. SF hydrogels were then washed with demineralized water and immersed in 10 mg $L^{-1}$ MB solutions. This way of pretreating the adsorbent before evaluating its adsorption capability was preferred to using the MB solution at various pH values. The latter situation may, indeed, induce a bias due to the adsorption competition between MB and hydroxide or proton ions. UV-vis spectrophotometry showed a pH-dependent MB adsorption. MB adsorption capacity increased with increasing the pH value of the pretreatment solution (Figure 5).

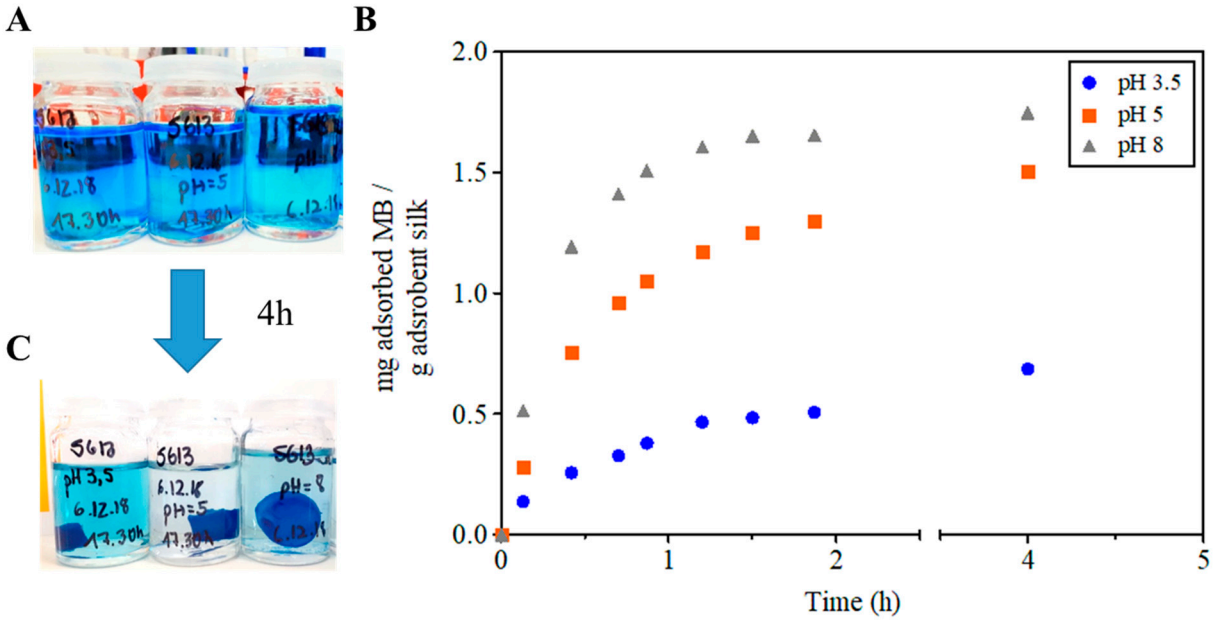


**Figure 5.** MB adsorption by SF hydrogels after three different pH treatments. Initial (**A**) and final (**C**) images of pH-treated silk hydrogels submerged in methylene blue solutions. From left to right, the pH treatments were 3.5, 5 and 8, respectively, in both images. Quantitative analysis of the mass of methylene blue adsorbed over time by UV-Vis spectrometry at 664 nm (**B**).

This result can be explained by the degree of swelling of the hydrogel. The pI of the heavy chain of SF has been described in the literature to be 4.4–4.5 [48]. Over this pH (pH = 8), the SF overall charge is negative due to the presence of carboxylate functions, while under this pH (pH = 3.5) carboxylates are protonated and therefore the hydrogel shrinks. Moreover, the changes induced within the SF hydrogel during the pH pretreatment are maintained when the hydrogel is placed in the MB solution. This effect may be due to kinetic considerations related to the diffusion of ions from the hydrogel to the surrounding solution. Accordingly, a pretreatment at pH = 3.5 may also influence the interaction between the hydrogel, expected to be positively charged, and MB, also positively charged. When the pH of the pretreatment solution increases, over the pI, SF materials become negatively charged, thus favoring the interaction with MB, which is positively charged.

### 3.3. Influence of the Ionic Strength of the Solution

Hydrogels were immersed in 0.6 M NaCl solutions for 48 h (see Figure 1). We chose the salt concentration corresponding to seawater salinity. After salt pretreatment, hydrogels considerably shrunk and became opaque (Figure 6A), probably due to the formation of a salt bridge between carboxylate and sodium ions. Interestingly, the immersion of this

material in aqueous solutions did not restore their original swelling state. After rinsing with demineralized water, samples were immersed in MB 10 mg $L^{-1}$ for 3 h. The pretreatment of hydrogels with salt resulted in a decrease in both the adsorption rate and the maximum adsorption capacity. This is clearly shown in Figure 6B through the lower slope, at an early stage, and the apparition of a plateau at the lower MB adsorbed mass.

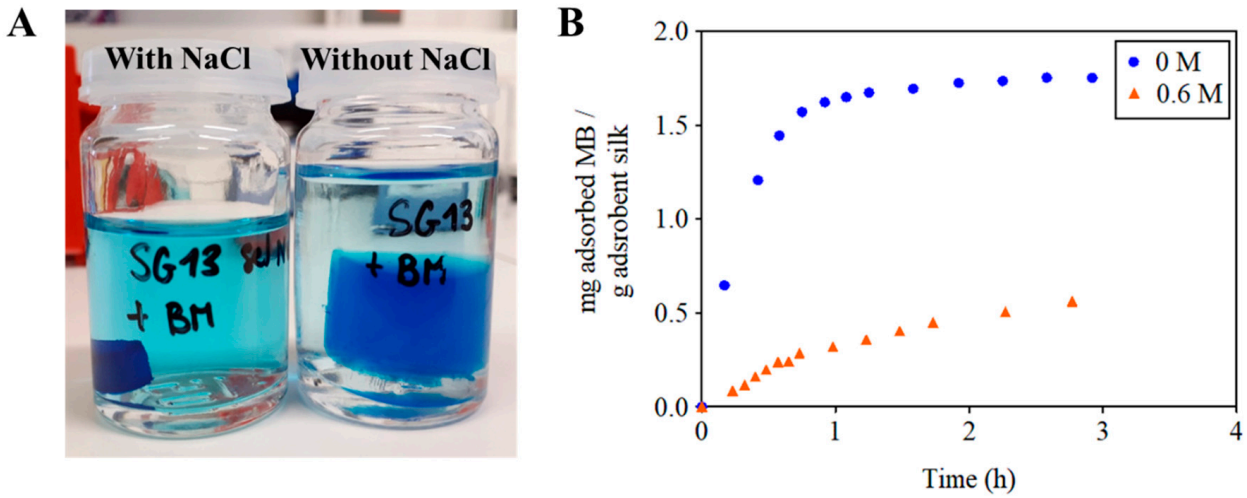


**Figure 6.** Images of sodium chloride treated (**left**) or not (**right**) SF hydrogels after MB adsorption (**A**). After salt pretreatment, the SF hydrogel was considerable shrunk. MB adsorption kinetics after sodium chloride pretreatment (**B**).

### *3.4. Brilliant Blue Adsorption*

Interestingly, the exact opposite adsorption behavior was observed when using brilliant blue (BB), an anionic dye, instead (Figure 7). In fact, BB was best adsorbed by hydrogels pretreated at pH 3. On the contrary, when hydrogels are pretreated at higher pH adsorption, the capacity decreased. Thus, though pH has an influence on hydrogel shrinking, the nature (anionic or cationic) of the dye also has an influence on its adsorption at a given pH. These results agree with the ones found in the literature when using silk/GO and silk/$TiO_2$ composite materials to adsorb different cationic and anionic dyes [11,49].

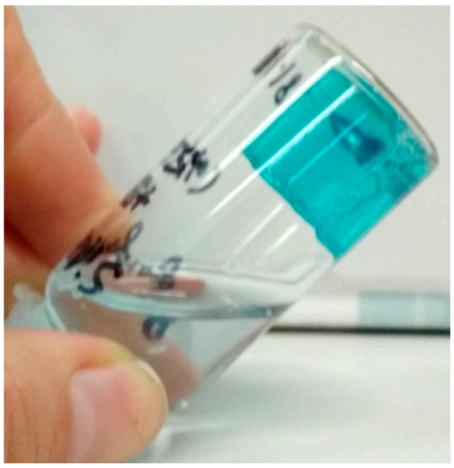

**Figure 7.** Brilliant Blue adsorption by SF hydrogel at pH 3. In contrast to MB, BB can be completely adsorbed at pH 3.

### *3.5. Adsorbent Regeneration and Recycling*

For successful application, adsorbent materials should not further pollute the environment by neither their production nor their degradation (methods and byproducts).

Therefore, biodegradable materials are of increasing interest in this field. In addition, the possibility to regenerate and recycle these materials increases their useful life, thus reducing their cost. The ability to regenerate and reuse SF materials has been evaluated in this section. Regeneration procedures should allow a maximum release of the adsorbed dye while preserving the adsorption capacity of the material. Herein, we investigated the release kinetics of the MB adsorbed in the materials in acid solution (pH 3).

MB-saturated materials were prepared by immersing them into MB solutions (10 mg $L^{-1}$) for 6 days. The immersion of MB-saturated SF materials into acid aqueous solution (pH = 3) resulted in a dye release into the solution (Figure 8A). This behavior agrees with the previously described effect of pH over SF materials. When SF materials are immersed in acid solutions, SF's overall charge becomes positive and electrostatic repulsion between SF and MB occurs, resulting in dye being released into the solution. By using this methodology, up to ~29% of the MB adsorbed by SF hydrogels was released into the solution (Figure 8B). The regenerated materials were then reused for MB adsorption conserving a ~70% of its initial adsorption capacity. After two cycles, the material was still useful, although its dye release capacity was reduced by ~30%. This reduction of the adsorption capacity could be explained by two hypotheses: (i) the saturation of several adsorption sites due to the incapacity of the material to release all the adsorbed MB molecules; and (ii) the hydrogel volume reduction induced by the acid solution treatment. This last effect was expected as the hydrogel tends to shrink in an acidic medium, as shown above. A combination of both hypotheses may also be possible; this deserves, however, further analyses to better understand the reason of this decrease over the adsorption capacity.

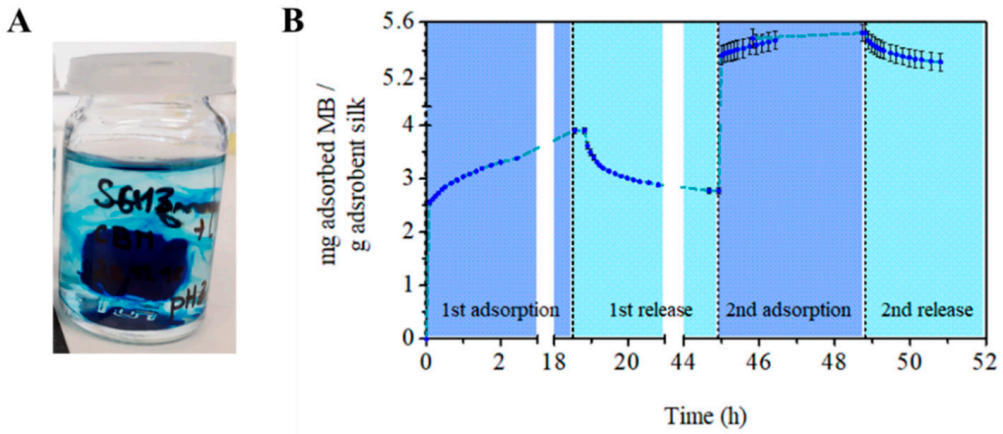


**Figure 8.** MB-saturated SF hydrogel immersion in pH 3 solution results in MB release (**A**). MB adsorption (pH 7) and release (pH 3) cycles by silk hydrogels (**B**).

### *3.6. MB Degradation by a SF-Au NPs Bionanocomposite*

In order to develop an adsorbent-based approach that can combine a non-pollutant adsorbent with an in situ degradation strategy we evaluate, as a proof-of-concept, the use of a silk fibroin hydrogel containing Au nanoparticles (SF-Au NPs bionanocomposite) for a combined adsorption and degradation of MB. The use of Au NPs as a catalyst has been largely studied in the literature [50–52]. Au NPs have been proved to catalyze the reduction of MB to leuco methylene blue (LMB, colorless) by sodium borohydride ($NaBH_4$) [34,53]. This reaction was chosen as a model reaction as it can be easily followed by UV-Vis measurements due to its blue color extinction. The combination of the MB adsorbent capacity with the catalytic activity of Au NPs can further be used in a continuous water treatment procedure. Not only Au NPs are able to degrade MB, but the direct contact of both elements is enhanced by the adsorption capacity of the SF material.

Figure 9B shows that, after only 15 min, all the MB had been reduced to LMB (see video x8 as supporting information). Control experiments were performed with hydrogels without Au NPs and if an adsorption of MB was observed, no degradation could be evidenced. Additionally, reduction of MB to LMB was successfully conducted with a

solution of Au NPs alone to confirm the catalytic role of Au NPs. In this later case, a small enhancement of the catalytical activity was evidenced (12 min rather than 15 min for a complete degradation in the same conditions). This result is expected because Au NPs are embedded within the hydrogel and the MB has to diffuse through the gel to reach the NPs.

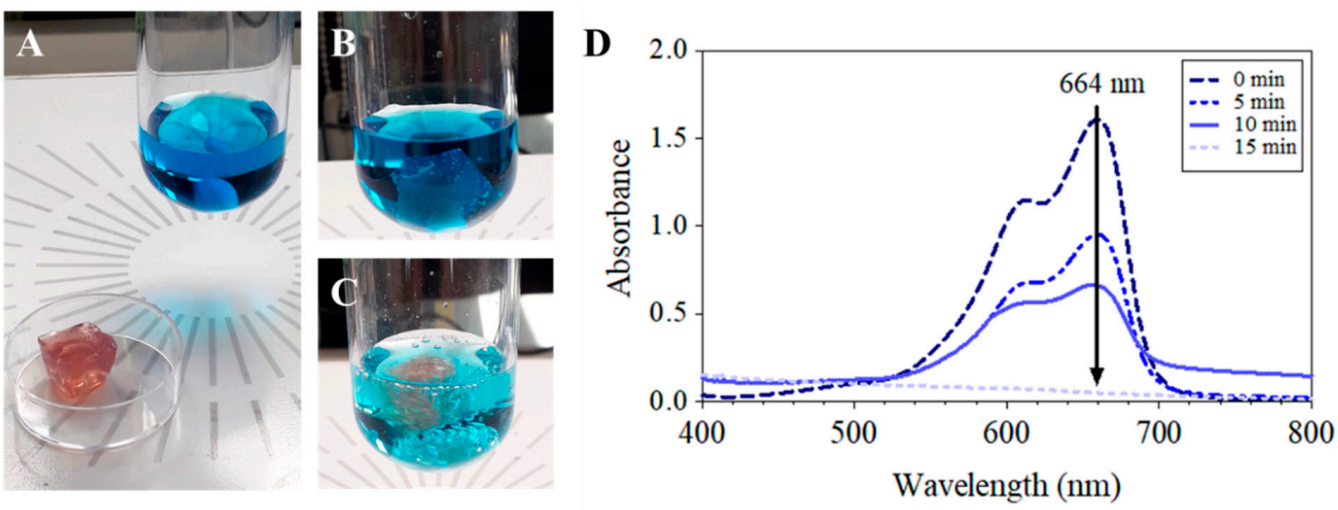


**Figure 9.** Silk-Au NPs hydrogel bionanocomposite and MB solution (**A**), image taken at the start (**B**) and during (**C**) MB reduction reaction. The formation of $H_2$ results in gas bubbles entrapped within the silk-Au NPs hydrogel. MB reduction kinetics monitored by UV-vis spectrophotometry (**D**).

Not only the reaction occurs in a relatively fast manner with SF-Au NPs bionanocomposite, but also the hydrogel can be reused by adding more MB and $NaBH_4$ at least up to 15 times resulting in the degradation of 5.9 µmol of MB by each µmol of Au NPs. Thus, it appears that MB is efficiently adsorbed by the SF-Au NPs composite and transformed into leuco MB by an electron transfer mechanism catalyzed by Au NPs [54,55]. We can hypothesize that the leuco MB, which is not charged, will have less affinity toward the silk adsorbent and be released then replaced by new MB molecules (see Figure 10).

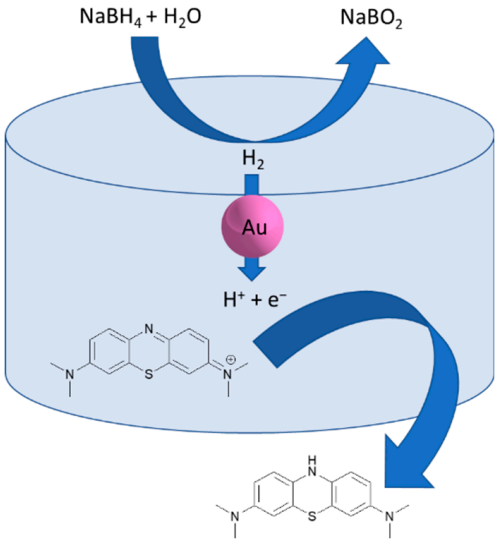


**Figure 10.** Scheme of the MB reduction by $NaBH_4$ catalyzed by AuNPs.

In spite of the great reduction of MB observed, the chosen reaction results in the production of hydrogen gas (coming from sodium borohydride) that is entrapped within the hydrogel (Figure 9A) resulting in a partial break down of the material after numerous reutilizations. Nevertheless, it should be noted that the NPs were attached to the remaining

SF fibers and no release into the solution was observed. These results on the lack of NPs release are in accord with the results that we have previously described [39]. These results are thus encouraging for the development of a non-pollutant and reusable system combining the MB adsorption and in situ degradation.

### *3.7. Comparison with Other Materials*

Many different materials are being developed for dye removal. Table 2 compiles some of these materials and their maximum adsorption capacities for MB. Although the results obtained within this work are largely outcome in some other cases presented in the literature, it is important to consider that these are only proof-of-concept results and further optimization of the materials should be conducted. Moreover, in the case of the adjunction to the silk hydrogels of a catalytical ability and reusability potency, the maximum removal capacity will be enhanced.

**Table 2.** Summary of MB removal materials and their maximum removal capacities.

| Material | Mode of Action | Maximum Capacity | Reference |
|---|---|---|---|
| SF hydrogel | Adsorption | 25.77 mg $g^{-1}$ | This work |
| Silk-graphene oxide aerogel | | 1322.71 mg $g^{-1}$ | [11] |
| Graphene oxide hydrogel | | 714.29 mg $g^{-1}$ | [10] |
| Alginate beads-magnetic NPs-activated carbon | | 18.23 mg $g^{-1}$ | [56] |
| Polyacrylamide dextran sulfate hydrogels | | 19.145 mg $g^{-1}$ | [41] |
| Exfoliated montmorillonite nanosheets-chitosan | | 530 mg $g^{-1}$ | [47] |
| SF-Au NPs hydrogel | Chemical reduction | | This work |
| Graphene-tanic acid-Au NPs hydrogel | | | [29] |

## 4. Conclusions

To our knowledge, the use of silk materials as adsorbents has rarely been studied to date. Herein, the maximum adsorption capacity of SF hydrogels has been evaluated. The better fit of the experimental data with the Langmuir adsorption model agrees with most of the studies on organic dye adsorption found in the literature. Moreover, the results found in this section strongly suggest an electrostatic-mediated interaction between MB and SF hydrogels. This interaction is in fact impaired in the presence of salt, or within an acid media due to the positive charge of SF materials at this stage. In addition, the use of an anionic dye resulted in an opposite behavior confirming the electrostatic interaction hypothesis. This work also shows the possibility of using pH 3 solutions to restore and reuse SF materials. Finally, the addition of Au NPs allows the coupling of the dye removal capacities of SF with its in-situ degradation by catalysis.

Herein, this work provides a biodegradable material capable of removing and degrading MB from an aqueous solution within a simple procedure. It is important to note that the results presented here are just a proof of concept and that the material can be easily tuned and functionalized to optimize its performance. Future investigations could focus on the use of HRP enzyme (used for hydrogel crosslinking) for pollutant degradation as recently shown in the literature [57] as well as their possible use in potential synergy with NPs catalyst.

**Supplementary Materials:** The following supporting information can be downloaded at: https://www.mdpi.com/article/10.3390/app12189152/s1, Video S1: methylene blue degradation in presence of NaBH4 and catalyzed by SF-AuNP (speed x8).

**Author Contributions:** Conceptualization, C.B.M. and E.G.; Formal analysis, C.B.M.; Funding acquisition, C.E., J.L. and E.G.; Methodology, C.B.M., C.E., J.L. and E.G.; Project administration, J.L. and E.G.; Supervision, J.L. and E.G.; Validation, C.E., J.L. and E.G.; Writing—original draft, C.B.M.; Writing—review & editing, J.L. and E.G. All authors have read and agreed to the published version of the manuscript.

**Funding:** This research received no external funding.

**Conflicts of Interest:** The authors declare no conflict of interest.

## References

1. Khan, S.; Malik, A. Toxicity Evaluation of Textile Effluents and Role of Native Soil Bacterium in Biodegradation of a Textile Dye. *Environ. Sci. Pollut. Res.* **2018**, *25*, 4446–4458. [CrossRef] [PubMed]
2. de Aragão Umbuzeiro, G.; Freeman, H.S.; Warren, S.H.; de Oliveira, D.P.; Terao, Y.; Watanabe, T.; Claxton, L.D. The Contribution of Azo Dyes to the Mutagenic Activity of the Cristais River. *Chemosphere* **2005**, *60*, 55–64. [CrossRef] [PubMed]
3. Verma, Y. Toxicity Assessment of Dye Containing Industrial Effluents by Acute Toxicity Test Using Daphnia Magna. *Toxicol. Ind. Health* **2011**, *27*, 41–49. [CrossRef] [PubMed]
4. Samanta, P.; Desai, A.V.; Let, S.; Ghosh, S.K. Advanced Porous Materials for Sensing, Capture and Detoxification of Organic Pollutants toward Water Remediation. *ACS Sustain. Chem. Eng.* **2019**, *7*, 7456–7478. [CrossRef]
5. Rajasulochana, P.; Preethy, V. Comparison on Efficiency of Various Techniques in Treatment of Waste and Sewage Water—A Comprehensive Review. *Resour.-Effic. Technol.* **2016**, *2*, 175–184. [CrossRef]
6. Jäger, I.; Hafner, C.; Schneider, K. Mutagenicity of Different Textile Dye Products in Salmonella Typhimurium and Mouse Lymphoma Cells. *Mutat. Res./Genet. Toxicol. Environ. Mutagenesis* **2004**, *561*, 35–44. [CrossRef] [PubMed]
7. Lellis, B.; Fávaro-Polonio, C.Z.; Pamphile, J.A.; Polonio, J.C. Effects of Textile Dyes on Health and the Environment and Bioremediation Potential of Living Organisms. *Biotechnol. Res. Innov.* **2019**, *3*, 275–290. [CrossRef]
8. Ghosh, D.; Bhattacharyya, K.G. Adsorption of Methylene Blue on Kaolinite. *Appl. Clay Sci.* **2002**, *20*, 295–300. [CrossRef]
9. Saravanan, A.; Senthil Kumar, P.; Jeevanantham, S.; Karishma, S.; Tajsabreen, B.; Yaashikaa, P.R.; Reshma, B. Effective Water/Wastewater Treatment Methodologies for Toxic Pollutants Removal: Processes and Applications towards Sustainable Development. *Chemosphere* **2021**, *280*, 130595. [CrossRef]
10. Pourjavadi, A.; Nazari, M.; Kabiri, B.; Hosseini, S.H.; Bennett, C. Preparation of Porous Graphene Oxide/Hydrogel Nanocomposites and Their Ability for Efficient Adsorption of Methylene Blue. *RSC Adv.* **2016**, *6*, 10430–10437. [CrossRef]
11. Wang, S.; Ning, H.; Hu, N.; Huang, K.; Weng, S.; Wu, X.; Wu, L.; Liu, J.; Alamusi. Preparation and Characterization of Graphene Oxide/Silk Fibroin Hybrid Aerogel for Dye and Heavy Metal Adsorption. *Compos. B Eng.* **2019**, *163*, 716–722. [CrossRef]
12. Ling, S.; Qin, Z.; Huang, W.; Cao, S.; Kaplan, D.L.; Buehler, M.J. Design and Function of Biomimetic Multilayer Water Purification Membranes. *Sci. Adv.* **2017**, *3*, e1601939. [CrossRef] [PubMed]
13. Xiao, S.; Wang, Z.; Ma, H.; Yang, H.; Xu, W. Effective Removal of Dyes from Aqueous Solution Using Ultrafine Silk Fibroin Powder. *Adv. Powder Technol.* **2014**, *25*, 574–581. [CrossRef]
14. Umar, M.; Min, K.; Jo, M.; Kim, S. Ultra-Thin, Conformal, and Hydratable Color-Absorbers Using Silk Protein Hydrogel. *Opt. Mater.* **2018**, *80*, 241–246. [CrossRef]
15. Godiya, C.B.; Cheng, X.; Deng, G.; Li, D.; Lu, X. Silk Fibroin/Polyethylenimine Functional Hydrogel for Metal Ion Adsorption and Upcycling Utilization. *J. Environ. Chem. Eng.* **2019**, *7*, 102806. [CrossRef]
16. Sato, T.; Abe, S.; Ito, S.; Abe, T. Silk Fibroin Fiber for Selective Palladium Adsorption: Kinetic, Isothermal and Thermodynamic Properties. *J. Environ. Chem. Eng.* **2019**, *7*, 102958. [CrossRef]
17. Gore, P.M.; Naebe, M.; Wang, X.; Kandasubramanian, B. Progress in Silk Materials for Integrated Water Treatments: Fabrication, Modification and Applications. *Chem. Eng. J.* **2019**, *374*, 437–470. [CrossRef]
18. Altman, G.H.; Diaz, F.; Jakuba, C.; Calabro, T.; Horan, R.L.; Chen, J.; Lu, H.; Richmond, J.; Kaplan, D.L. Silk-Based Biomaterials. *Biomaterials* **2003**, *24*, 401–416. [CrossRef]
19. Ebrahimi, D.; Tokareva, O.; Rim, N.G.; Wong, J.Y.; Kaplan, D.L.; Buehler, M.J. Silk-Its Mysteries, How It Is Made, and How It Is Used. *ACS Biomater. Sci. Eng.* **2015**, *1*, 864–876. [CrossRef]
20. Belanger, K.; Schlatter, G.; Hébraud, A.; Marin, F.; Testelin, S.; Dakpé, S.; Devauchelle, B.; Egles, C. A Multi-Layered Nerve Guidance Conduit Design Adapted to Facilitate Surgical Implantation. *Health Sci. Rep.* **2018**, *1*, e86. [CrossRef]
21. Yang, Y.; Chen, X.; Ding, F.; Zhang, P.; Liu, J.; Gu, X. Biocompatibility Evaluation of Silk Fibroin with Peripheral Nerve Tissues and Cells in Vitro. *Biomaterials* **2007**, *28*, 1643–1652. [CrossRef] [PubMed]
22. Fernández-García, L.; Marí-Buyé, N.; Barios, J.A.; Madurga, R.; Elices, M.; Pérez-Rigueiro, J.; Ramos, M.; Guinea, G.V.; González-Nieto, D. Safety and Tolerability of Silk Fibroin Hydrogels Implanted into the Mouse Brain. *Acta Biomater.* **2016**, *45*, 262–275. [CrossRef] [PubMed]
23. Kundu, S.C. *Silk Biomaterials for Tissue Engineering and Regenerative Medicine*; Woodhead Publishing: Cambridge, UK, 2014. [CrossRef]
24. Belda Marín, C.; Fitzpatrick, V.; Kaplan, D.L.; Landoulsi, J.; Guénin, E.; Egles, C. Silk Polymers and Nanoparticles: A Powerful Combination for the Design of Versatile Biomaterials. *Front. Chem.* **2020**, *8*, 604398. [CrossRef]

25. Gao, X.; Gou, J.; Zhang, L.; Duan, S.; Li, C. A Silk Fibroin Based Green Nano-Filter for Air Filtration. *RSC Adv.* **2018**, *8*, 8181–8189. [CrossRef]
26. Trueman, H.E.; Sriskantha, A.; Qu, Y.; Rapson, T.D.; Sutherland, T.D. Modification of Honeybee Silk by the Addition of Antimicrobial Agents. *ACS Omega* **2017**, *2*, 4456–4463. [CrossRef] [PubMed]
27. Horgan, C.C.; Han, Y.S.; Trueman, H.; Jackson, C.J.; Sutherland, T.D.; Rapson, T.D. Phosphorescent Oxygen-Sensing and Singlet Oxygen Production by a Biosynthetic Silk. *RSC Adv.* **2016**, *6*, 39530–39533. [CrossRef]
28. Ania, C.O.; Menéndez, J.A.; Parra, J.B.; Pis, J.J. Microwave-Induced Regeneration of Activated Carbons Polluted with Phenol. A Comparison with Conventional Thermal Regeneration. In *Carbon*; Elsevier Ltd.: Amsterdam, The Netherlands, 2004; Volume 42, pp. 1383–1387. [CrossRef]
29. Luo, J.; Zhang, N.; Lai, J.; Liu, R.; Liu, X. Tannic Acid Functionalized Graphene Hydrogel for Entrapping Gold Nanoparticles with High Catalytic Performance toward Dye Reduction. *J. Hazard. Mater.* **2015**, *300*, 615–623. [CrossRef] [PubMed]
30. Wang, T.; Su, J.; Jin, X.; Chen, Z.; Megharaj, M.; Naidu, R. Functional Clay Supported Bimetallic NZVI/Pd Nanoparticles Used for Removal of Methyl Orange from Aqueous Solution. *J. Hazard. Mater.* **2013**, *262*, 819–825. [CrossRef]
31. Wang, M.; Yang, Y.; Long, J.; Mao, Z.; Qiu, T.; Wu, Q.; Chen, X. Synthesis of Pt3Ni Microspheres with High Performance for Rapid Degradation of Organic Dyes. *Nanoscale Res. Lett.* **2015**, *10*, 236. [CrossRef]
32. Vanaja, M.; Paulkumar, K.; Baburaja, M.; Rajeshkumar, S.; Gnanajobitha, G.; Malarkodi, C.; Sivakavinesan, M.; Annadurai, G. Degradation of Methylene Blue Using Biologically Synthesized Silver Nanoparticles. *Bioinorg. Chem. Appl.* **2014**, *2014*, 742346. [CrossRef]
33. Barroso-Martín, I.; Moretti, E.; Talon, A.; Storaro, L.; Rodríguez-Castellón, E.; Infantes-Molina, A. Au and AuCu Nanoparticles Supported on SBA-15 Ordered Mesoporous Titania-Silica as Catalysts for Methylene Blue Photodegradation. *Materials* **2018**, *11*, 890. [CrossRef] [PubMed]
34. Begum, R.; Najeeb, J.; Sattar, A.; Naseem, K.; Irfan, A.; Al-Sehemi, A.G.; Farooqi, Z.H. Chemical Reduction of Methylene Blue in the Presence of Nanocatalysts: A Critical Review. *Rev. Chem. Eng.* **2019**, *36*, 749–770. [CrossRef]
35. Najahi-Missaoui, W.; Arnold, R.D.; Cummings, B.S. Safe Nanoparticles: Are We There Yet? *Int. J. Mol. Sci.* **2020**, *22*, 385. [CrossRef]
36. Carnovale, C.; Bryant, G.; Shukla, R.; Bansal, V. Identifying Trends in Gold Nanoparticle Toxicity and Uptake: Size, Shape, Capping Ligand, and Biological Corona. *ACS Omega* **2019**, *4*, 242–256. [CrossRef]
37. Aufaure, R.; Buendia, R.; Motte, L.; Hardouin, J.; Lalatonne, Y.; Guénin, E. Versatile "Click" Synthesis of 1-Hydroxy-1,1-Methylenebisphosphonic Acids with Thioalkoxy Substituents for the Preparation of Stable Gold Nanoparticles. *New J. Chem.* **2017**, *41*, 12153–12158. [CrossRef]
38. Rockwood, D.N.; Preda, R.C.; Yücel, T.; Wang, X.; Lovett, M.L.; Kaplan, D.L. Materials Fabrication from Bombyx Mori Silk Fibroin. *Nat. Protoc.* **2011**, *6*, 1612–1631. [CrossRef] [PubMed]
39. Belda Marín, C.; Egles, C.; Humblot, V.; Lalatonne, Y.; Motte, L.; Landoulsi, J.; Guénin, E. Gold, Silver, and Iron Oxide Nanoparticle Incorporation into Silk Hydrogels for Biomedical Applications: Elaboration, Structure, and Properties. *ACS Biomater. Sci. Eng.* **2021**, *7*, 2358–2371. [CrossRef]
40. Partlow, B.P.; Hanna, C.W.; Rnjak-Kovacina, J.; Moreau, J.E.; Applegate, M.B.; Burke, K.A.; Marelli, B.; Mitropoulos, A.N.; Omenetto, F.G.; Kaplan, D.L. Highly Tunable Elastomeric Silk Biomaterials. *Adv. Funct. Mater.* **2014**, *24*, 4615–4624. [CrossRef]
41. Perju, M.M.; Dinu, M.V.; Dragan, E.S. Sorption of Methylene Blue onto Ionic Composite Hydrogels Based on Polyacrylamide and Dextran Sulfate: Kinetics, Isotherms, and Thermodynamics. *Sep. Sci. Technol.* **2012**, *47*, 1322–1333. [CrossRef]
42. Filho, C.M.C.; Bueno, P.V.A.; Matsushita, A.F.Y.; Rubira, A.F.; Muniz, E.C.; Durães, L.; Murtinho, D.M.B.; Valente, A.J.M. Synthesis, Characterization and Sorption Studies of Aromatic Compounds by Hydrogels of Chitosan Blended with β-Cyclodextrin- and PVA-Functionalized Pectin. *RSC Adv.* **2018**, *8*, 14609–14622. [CrossRef]
43. Batool, F.; Akbar, J.; Iqbal, S.; Noreen, S.; Bukhari, S.N.A. Study of Isothermal, Kinetic, and Thermodynamic Parameters for Adsorption of Cadmium: An Overview of Linear and Nonlinear Approach and Error Analysis. *Bioinorg. Chem. Appl.* **2018**, *2018*. [CrossRef] [PubMed]
44. Daryabeigi Zand, A.; Rabiee Abyaneh, M. Adsorption of Lead, Manganese, and Copper onto Biochar in Landfill Leachate: Implication of Non-Linear Regression Analysis. *Sustain. Environ. Res.* **2020**, *30*, 18. [CrossRef]
45. Sinha, V.; Chakma, S. Advances in the Preparation of Hydrogel for Wastewater Treatment: A Concise Review. *J. Environ. Chem. Eng.* **2019**, *7*, 103295. [CrossRef]
46. Putro, J.N.; Kurniawan, A.; Ismadji, S.; Ju, Y.H. Nanocellulose Based Biosorbents for Wastewater Treatment: Study of Isotherm, Kinetic, Thermodynamic and Reusability. *Environ. Nanotechnol. Monit. Manag.* **2017**, *8*, 134–149. [CrossRef]
47. Kang, S.; Zhao, Y.; Wang, W.; Zhang, T.; Chen, T.; Yi, H.; Rao, F.; Song, S. Removal of Methylene Blue from Water with Montmorillonite Nanosheets/Chitosan Hydrogels as Adsorbent. *Appl. Surf. Sci.* **2018**, *448*, 203–211. [CrossRef]
48. Foo, C.W.P.; Bini, E.; Hensman, J.; Knight, D.P.; Lewis, R.V.; Kaplan, D.L. Role of PH and Charge on Silk Protein Assembly in Insects and Spiders. *Appl. Phys. A Mater. Sci. Process.* **2006**, *82*, 223–233. [CrossRef]
49. Aziz, S.; Sabzi, M.; Fattahi, A.; Arkan, E. Electrospun Silk Fibroin/PAN Double-Layer Nanofibrous Membranes Containing Polyaniline/TiO2 Nanoparticles for Anionic Dye Removal. *J. Polym. Res.* **2017**, *24*, 140. [CrossRef]
50. Xie, J.; Yang, X.; Xu, X. Wet Chemical Method for Synthesizing 3D Graphene/Gold Nanocomposite: Catalytic Reduction of Methylene Blue. *Phys. E Low Dimens. Syst. Nanostruct.* **2017**, *88*, 201–205. [CrossRef]

51. León, E.R.; Rodríguez, E.L.; Beas, C.R.; Plascencia-Villa, G.; Palomares, R.A.I. Study of Methylene Blue Degradation by Gold Nanoparticles Synthesized within Natural Zeolites. *J. Nanomater.* **2016**, *2016*, 9541683. [CrossRef]
52. Zhang, Y.; Cui, X.; Shi, F.; Deng, Y. Nano-Gold Catalysis in Fine Chemical Synthesis. In *Chemical Reviews*; American Chemical Society: Washington, DC, USA, 2012; pp. 2467–2505. [CrossRef]
53. Islam, M.T.; Dominguez, N.; Ahsan, M.A.; Dominguez-Cisneros, H.; Zuniga, P.; Alvarez, P.J.J.; Noveron, J.C. Sodium Rhodizonate Induced Formation of Gold Nanoparticles Supported on Cellulose Fibers for Catalytic Reduction of 4-Nitrophenol and Organic Dyes. *J. Environ. Chem. Eng.* **2017**, *5*, 4185–4193. [CrossRef]
54. Ganapuram, B.R.; Alle, M.; Dadigala, R.; Dasari, A.; Maragoni, V.; Guttena, V. Catalytic Reduction of Methylene Blue and Congo Red Dyes Using Green Synthesized Gold Nanoparticles Capped by Salmalia Malabarica Gum. *Int. Nano Lett.* **2015**, *5*, 215–222. [CrossRef]
55. Lukhele, E.J.; Khutlane, J.T.; Báthori, N.B.; Malgas-Enus, R. Reduction and Removal of Methylene Blue from Aqueous Solutions via Recyclable Magnetic Gold Nanomaterials. *Surf. Interfaces* **2022**, *31*, 101970. [CrossRef]
56. Rocher, V.; Siaugue, J.M.; Cabuil, V.; Bee, A. Removal of Organic Dyes by Magnetic Alginate Beads. *Water Res.* **2008**, *42*, 1290–1298. [CrossRef] [PubMed]
57. Šekuljica, N.; Prlainović, N.; Stefanović, A.B.; Žuža, M.G.; Čičkarić, D.Z.; Mijin, D.; Knezevic-Jugovic, Z.D. Decolorization of Anthraquinonic Dyes from Textile Effluent Using Horseradish Peroxidase: Optimization and Kinetic Study. *Sci. World J.* **2015**, *2015*, 371625. [CrossRef]